

Received March 4, 2021, accepted March 28, 2021, date of publication April 7, 2021, date of current version April 14, 2021.

Digital Object Identifier 10.1109/ACCESS.2021.3071639

Location-Based Vertical Handovers in Wi-Fi Networks With IEEE 802.11ah

SERENA SANTI¹, (Graduate Student Member, IEEE), TOBIA DE KONINCK¹,
GLENN DANEELS¹, FILIP LEMIC¹, AND JEROEN FAMAËY¹, (Senior Member, IEEE)

Internet and Data Lab (IDLab), University of Antwerp - IMEC, 2000 Antwerp, Belgium

Corresponding author: Serena Santi (serena.santi@uantwerpen.be)

This work was supported by the Flemish IDEAL-IoT project (FWO SBO) under Grant S004017N. The work of Serena Santi was supported by the Flemish FWO SB Grant 1S82120N. The work of Filip Lemic was supported by the EU Marie Skłodowska Curie Actions (MSCA) under Grant 893760.

ABSTRACT IEEE 802.11ah is a new sub-GHz Wi-Fi technology that provides several advantages over traditional Wi-Fi such as a higher communication range, enhanced scalability, and lower energy consumption, however at the cost of substantially lower throughput. With the aim of simultaneously benefiting from multiple Wi-Fi technologies, recent proposals suggest combining a number of these technologies into a single device. This, however, compromises the energy efficiency of the device, as it implies concurrent utilization of different radio access interfaces. To mitigate this issue, the device should utilize the interface of a certain technology only when there is a high probability of establishing communication over that technology. Traditional vertical handover algorithms are not designed for this purpose as they rely on continuous beacon listening or active probing, even if the device is not in the range of a given technology. To address this issue, vertical handover algorithms based on the combination of devices' physical locations and either Radio Environmental Maps (REM) or propagation modeling have been proposed. Moreover, their suitability and encouraging performance have been demonstrated for a number of the established Low-Power Wide-Area Network (LPWAN) technologies. However, their appropriateness for Wi-Fi-based networks with IEEE 802.11ah is currently unknown, which provides the main motivation for this work. Specifically, we carry out an extensive experimental performance evaluation of two location-based vertical handover algorithms in the context of Wi-Fi-based networks with IEEE 802.11ah. Our results demonstrate the feasibility of location-based handovers in this context. We base our findings on the fact that location-based algorithms can maintain comparable data communication quality as the beacon listening-based baseline, while simultaneously reducing the utilization of the IEEE 802.11ah and IEEE 802.11n radio access interfaces by a factor of 2 and 10, respectively.

INDEX TERMS Wi-Fi, IEEE 802.11ah, Low-Power Wide-Area Network, vertical handover, location-awareness, Radio Environmental Map

I. INTRODUCTION

In recent years, we are witnessing an explosion in the number of Low-Power Wide-Area Network (LPWAN)-enabled devices. The new IEEE 802.11ah standard [1] is interesting in this context, mainly because it is considered as both an LPWAN and Wi-Fi technology. It features a communication range of up to 1 kilometer and provides megabits per second data-rates [2]. It also offers higher energy efficiency and scalability, as it is able to simultaneously establish connections

The associate editor coordinating the review of this manuscript and approving it for publication was Wei-Wen Hu¹.

from a single Access Point (AP) to more than 8000 stations [3], [4]. On the other end, traditional Wi-Fi technologies offer higher data-rates, however their communication range is limited to tens of meters and their energy efficiency and scalability is significantly lower compared to IEEE 802.11ah.

Intuitively, many applications would benefit from the longer range and the energy efficiency of one technology combined with higher throughput of the other. To enable that, several multi-Radio Access Technology (RAT) devices have been proposed, especially in the LPWAN context, with one prominent example being [5]. Such multi-RAT devices will have to utilize a certain algorithm for deciding if a handover

from one technology to another should be performed, which is referred to as “vertical handover”. Traditional vertical handover algorithms rely on the device listening for beacons periodically transmitted by the nearby APs [6]. Adversely, the device can utilize active probing for discovering nearby APs of a certain technology. Both procedures consume excessive amounts of energy, as the beacon listening or active probing has to be performed even if the device is far from the coverage region of the technology. This is a highly undesirable, especially for LPWAN-enabled Internet of Things (IoT) devices targeting low-power performance.

This design limitation of traditional vertical handover algorithms has been recognized in the LPWAN community. One important realization is that many LPWAN-supported IoT use-cases require knowledge of the device’s location, thus many LPWAN devices utilize either the Global Positioning System (GPS) or the LPWAN network itself for determining their locations [6]. Hence, the location of the device can be used to perform LPWAN availability discovery to support energy efficient vertical handovers. This intuition resulted in several proposals for location-based handover, with arguably the two most prominent examples being based on the combination of i) the Station (STA)’s location and a Radio Environmental Map (REM) [7] and ii) the STA’s and AP’s locations and propagation modeling [6]. The feasibility of these handover algorithms has been demonstrated in the broad context of LPWANs [6].

However, the feasibility of location-based vertical handovers is currently unclear in the context of Wi-Fi based networks, especially those including IEEE 802.11ah, primarily due to the novelty of the technology and the absence of hardware on the market. Therefore, the main aim of this paper is to close this gap. Specifically, in this work we experimentally evaluate the performance of the two aforementioned location-based algorithms, as well as compare their performance with the performance of a more traditional baseline based on beacon listening. We focus our study on IEEE 802.11ah and IEEE 802.11n primarily due to the fact that these technologies naturally integrate well as they are both Wi-Fi-based. One realistic example where such a setup can be useful stems from the idea of using IEEE 802.11ah as the technology providing seamless connectivity, while IEEE 802.11n could be used for data intensive tasks such as data offloading or firmware update [5]. We derive our insights using experimental measurements collected in a realistic outdoor setup. The obtained results show that location-based handovers in the context of Wi-Fi networks with IEEE 802.11ah are generally feasible and their performance is encouraging. Our conclusions are based on the fact that the location-based handover algorithms significantly outperform the baseline in terms of energy consumption, while at the same time maintaining comparable quality of data communication.

The remainder of this paper is structured as follows. In the next section, we overview the existing literature on IEEE 802.11ah and vertical handovers in LPWANs. Moreover, in Section III we provide an overview of the considered

vertical handover algorithms. In Section IV, we discuss the measurement collection, as well as the utilized methodology for evaluating the performance of the considered algorithms. Section V provides the performance results and observed insights. Finally, in Section VI we conclude the paper and provide several directions for future research.

II. RELATED WORK

A. OVERVIEW OF IEEE 802.11ah

Due to the novelty of the LPWAN technology considered in this work (i.e., IEEE 802.11ah), we see it beneficial to summarize its main features. LPWANs are wireless networks in which devices can communicate over long ranges at low data rates and high energy efficiency. Examples of LPWAN technologies are NB-IoT, LoRa, Sigfox, IEEE 802.11ah, IEEE 802.15.4g, etc. [2], [8]. These technologies widely differ in terms of bandwidth, range, data rate, payload size, and transmission power, although their common goals are to provide long range and to be energy efficient.

The novel IEEE 802.11ah, also known as Wi-Fi Halow, has the unique advantage of being built upon the omnipresent Wi-Fi technology. IEEE 802.11ah utilizes the sub-GHz Industrial, Scientific, and Medical (ISM) frequency band (in contrast to IEEE 802.11n utilizing 2.4 and 5 GHz ISM frequencies). The maximum bandwidth used by IEEE 802.11ah is 16 MHz, i.e., less than the bandwidth of IEEE 802.11n equaling to 20 MHz or more. The Media Access Control (MAC) layer of IEEE 802.11ah has been adapted to support 8000 stations (in contrast to 2007 supported by IEEE 802.11n [9]), as well as to reduce the energy efficiency and the overhead of many short packets typical for LPWAN deployments. To reduce the overhead, IEEE 802.11ah features novel frame headers, user grouping mechanisms, medium access restrictions, and association and authentication mechanisms. More details are given in e.g., [3], [10].

B. LOCATION-BASED VERTICAL HANDOVER

Location-based optimizations in wireless networks show a great promise in advancing the network performance across all layers of their protocol stacks [11]. In terms of network handovers (both horizontal and vertical), location-awareness has been shown to be feasible and often highly beneficial in cellular and Local-Area Networks (LANs). For example, the authors in [12] ground the horizontal and vertical handover decisions on the location information of the STA in cognitive cellular networks. In addition, location-assisted handover procedures focused on IEEE 802.11 networks have been proposed in [13] and [14]. Both approaches base the selection of the potential next AP on the geographical region of the STA. In [15], the authors propose a procedure for data offloading from cellular networks to IEEE 802.11 hotspots (i.e., vertical handover), where the procedure utilizes current and future locations of the STA for deciding when and how much traffic to offload. While the previously discussed selected efforts

demonstrate the promise of location-based vertical handovers in cellular and/or traditional 802.11-based networks, in this work we focus on LPWAN technologies in which the energy consumption and duty-cycle constraints are stringent, hence their optimizations are even more relevant.

LPWAN-focused vertical handovers received substantially less attention from the research community to date, primarily due to their relatively recent emergence. In addition, the low power nature of LPWAN-enabled devices, combined with rather large deployment environments, pose additional challenges for location-based vertical handovers. Mainly due to the large sizes of LPWAN deployment environments, it is possible and to be expected that the GPS accuracy of location information will change dynamically and be better in e.g., urban canyons than in open spaces. In addition and mainly due to the low power nature of LPWAN-enabled devices, it is possible that GPS cannot be used for determining location of the devices, as it consumes relatively high amounts of energy. Hence, alternative localization sources are potentially needed for localizing the devices (e.g., utilizing LPWAN [16], [17] or Frequency Modulation (FM) radio signals [18] for localization purposes), which feature localization errors between one and two orders of magnitude higher than the GPS [19].

These issues have been relatively recently recognized in the research community. Specifically, the authors in [6] provide an approach for location-based discovery and handover of LPWAN technologies in outdoor environments. In this approach, the decision on when to perform a vertical handover between LPWAN technologies is based on the physical locations of the STA and the APs. By utilizing the locations and some knowledge about the environment of interest, the system is able to determine the expected Signal-to-Noise Ratio (SNR) between the devices, which is then used for deciding if the handover should at all be initiated. Adversely, the decision can be based only on the location of the STA combined with the preexisting REM [7], or by combining locations, SNR modeling, and sparse REMs [20]. The approach presented in [6] is able to explicitly and dynamically account for the inaccuracies in the estimated location of the STA. This allows it to account for different types of localization services to be used for generating location information, as well for sudden and temporary degradations in the quality of location information provisioning that could occur when the STA is entering a building, tunnels, urban canyons, etc. In addition, the proposed approach allows for internal tuning of the performance of vertical handover, which in turn provides a straightforward way of dealing with design trade-offs between energy consumption on the one hand, and communication ranges and handover delay on the other.

Due to the above-mentioned design advantages of location-based vertical handover outlined in [6], different flavors of this algorithm have been evaluated for established LPWAN technologies such as Sigfox and LoRa [6], as well as for the combination of NB-IoT and IEEE 802.11ah, though the latter solely in the form of a simulation-based study [21]. These studies generally suggest highly promising performance of

the location-based vertical handover, especially for LPWAN technologies for which energy efficiency is among the primary concerns. In contrast to the majority of the efforts mentioned above, we focus on IEEE 802.11ah, which per se is novel and for which the feasibility and performance of vertical handover algorithms is currently unclear. Moreover and to the best of our knowledge, this is the first work examining the interplay between vertical handovers among two Wi-Fi-based technologies, with one being a representative of LPWANs (i.e., IEEE 802.11ah), while the other representing a traditional Wireless LAN (WLAN) (i.e., IEEE 802.11n). Such a combination, although seemingly natural due to the seamlessness of Wi-Fi, has received very little attention from the community to date. Finally, we carry out our evaluation using experimental measurements collected in a realistic setup relevant for both technologies (e.g., the aforementioned data offloading and firmware update scenario), which is in contrast to contemporary IEEE 802.11ah-focused studies that are predominantly simulation-based (e.g., [21]).

III. VERTICAL HANDOVER ALGORITHMS

This section provides a short overview of the vertical handover algorithms considered in this work. The pseudo-code of the algorithms is given in the Appendix.

A. BEACON LISTENING-BASED VERTICAL HANDOVER

The first considered algorithm is based on traditional beacon listening [1], [21] and is, therefore, considered as the baseline algorithm for this work. In Algorithm 1 (cf., Appendix), beacons are periodically transmitted by an AP with a fixed amount of time between them. Upon waking up to listen for beacons, if a beacon is received the device can start the association procedure. This basic version of the algorithm is based on dropping the communication link even if a single beacon is missed [21]. However, due to the fact that the operational frequencies in IEEE 802.11ah and IEEE 802.11n are in the license-free frequency bands, there are various other technologies expected to operate in these frequency bands. Therefore, experiencing a connectivity loss (i.e., a beacon missed) for a short period is expected, especially toward the edge of the network. To prevent frequently re-associating after disconnection due to missing a single beacon, our algorithm is modified to allow up to β missed beacons, as shown in Algorithm 1. A major intuitive drawback of the presented algorithm is that the radio access interfaces of both technologies have to be periodically turned on even if the device is not in their coverage regions, resulting in unnecessary energy consumption.

B. LOCATION-BASED VERTICAL HANDOVER

This algorithm utilizes the location of the STA and APs deployed in an environment of interest and was first introduced in [6]. The assumption here is that APs are generally static, thus their exact physical locations can be pre-determined. Moreover, for localization the STA the authors suggest the usage of standard IoT localization approaches

(e.g., GPS). Based on the distance between the STA and each of the APs and some knowledge about the environment of interest (i.e., average path loss as the basic requirement) the algorithm is able to estimate the expected SNR between each AP and the STA. If the expected SNR is higher than a desired SNR threshold, the algorithm decides that a vertical handover should be performed. Only in that case the radio access interface of that technology are turned on and the link establishment is attempted. Intuitively, this mitigates the unnecessary beacon listening or active probing in case there is only a small or no probability of the device being in the coverage region of a certain technology. The approach is formally described in Algorithm 2. Similar as before, the algorithm allows missing up to β beacons before disconnecting from the network. This allows the SNR to have a short dip, preventing frequent re-associations directly after disconnections.

To estimate the SNR based on the devices' locations and without using an REM, the authors in [6] suggest the usage of propagation modeling. The suitability of different propagation models for IEEE 802.11ah was established as a part of our previous work [22]. Specifically, in [22] we evaluated the suitability of a set of propagation models for IEEE 802.11ah in three distinct types of environments (i.e., outdoor urban, outdoor rural, indoor). The following channel models were considered: COST-231 Hata [23], COST-231 Walfisch-Ikegami [23], ITU-R Below Rooftop [24], IEEE 802.11ah Macro, IEEE 802.11ah Micro, and IEEE 802.11ah Indoor models [25]. The best performing propagation model, namely COST-231 Hata, is exclusively used here, as it was shown to perform best in the environment considered in this work.

C. REM-BASED VERTICAL HANDOVER

In contrast to using propagation modeling, one could resort to using an REM in case of its availability for a given environment of interest. The algorithm discussed in this section assumes the existence of an REM which maps physical locations in an environment to the SNR observed at these locations (e.g., through surveying or crowd-sourcing [22]). Similar as before, the algorithm decides to initiate the handover only if the SNR at a given location is below a certain threshold, as shown in Algorithm 3. Note that this algorithm is also a location-based one, as it requires the current location of the STA for correlating it with the SNR from the REM database. Nonetheless, in the remainder of the paper we will refer to it as “REM-based algorithm” in order to provide a clear separation from the “Location-based algorithm” discussed previously. Similar to the location-based algorithm, the REM-based one allows the radio access interfaces to be turned off if the probability of the given technologies being available is too small. However and in contrast to the location-based algorithm, this algorithm requires the REM, which is often challenging to generate (especially for relatively large areas covered by LPWAN networks) and becomes stale over time, posing an additional maintenance overhead [20]. Finally, we used a suitable dataset from [22] for populating

the REM database needed for enabling this algorithm in the environment considered in this work.

IV. MEASUREMENT METHODOLOGY

In this section, we provide an overview of the methodology used for establishing the performance of the considered algorithms. First, we discuss the hardware setup used during the measurement campaign. Second, we overview the measurement collection procedure, as well as the features of the collected measurements. Third, we discuss the intuition behind our emulation-based evaluation approach based on combining the experimentally collected measurements with simulated mobility of the STA. Finally, we discuss the performance metrics considered in the evaluation.

A. HARDWARE SETUP

The hardware setup used for the measurement collection is shown in Figure 1. The setup consists of the following:

- 4 OpenMote B nodes whose sub-GHz radio (i.e., Atmel AT86RF215) is used to “mimic” the IEEE 802.11ah physical layer, as no official hardware is currently available on the market (more details below). These nodes are connected to either a Raspberry Pi or laptop, as shown in the figure. All the devices are configured to transmit at maximum transmission power of 14.5 dBm. The sub-GHz radio of the OpenMote B nodes feature theoretical receiver sensitivities of -123 dBm [26], although no signals were received with Received Signal Strength Indicator (RSSI) below -115 dBm. We use four motes (with each device having a separate mode for RX and TX) purely to speed-up the measurement campaign, acknowledging that the setup can be made operational with two nodes only.
- Raspberry Pi that supports IEEE 802.11n connectivity through its built-in IEEE 802.11n radio. Two OpenMote B motes are connected to the Raspberry Pi for enabling IEEE 802.11ah connectivity. The Adafruit GPS Hat is used for obtaining the current location of the STA, as shown in the figure.
- Wi-Fi AP is used for establishing IEEE 802.11n links, specifically a Routerboard RB951G-2HnD operating in the 2.4 GHz ISM band.
- A laptop is used for connecting two of the previously mentioned OpenMote B motes in order to transmit and receive IEEE 802.11ah packets. By connecting the laptop to the Wi-Fi AP using an Ethernet connection, the setup is also able to send packets over IEEE 802.11n.

The laptop, Wi-Fi AP, and two OpenMote B motes form the server (or the “access point”) part of the setup at a fixed location and powered through the electricity grid. As the Raspberry Pi and two OpenMote B nodes are being positioned at different locations within the measurement area, these are powered by a power bank, as indicated in the figure. The mobile part of the setup is held by a person walking around the measurement environment, while the receiving

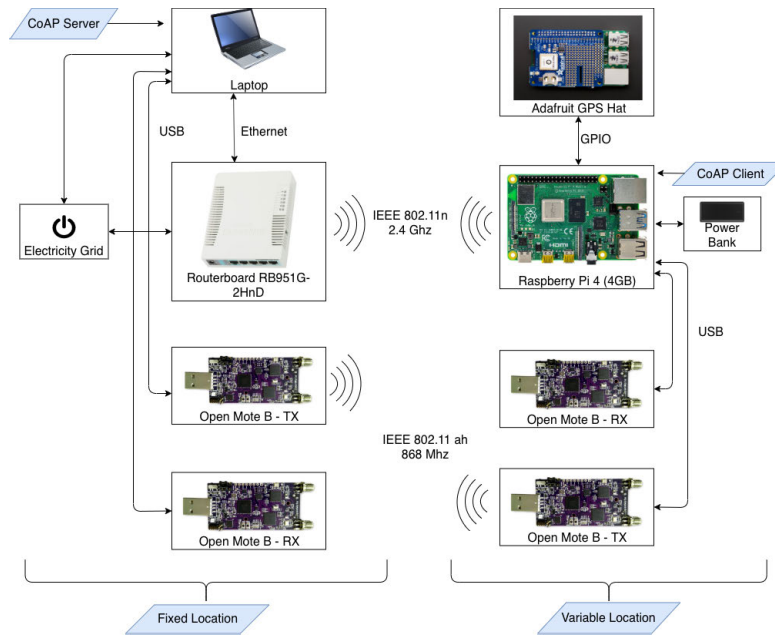


FIGURE 1. Measurement campaigns.

module is placed on a pole at 1.5 m above the ground, logging the collected measurements. All OpenMote B nodes run a program adapted from the OpenWSN project [27].

As mentioned, for enabling IEEE 802.11ah communication we used the Atmel AT86RF215 sub-GHz radio of the OpenMote B nodes that are originally designed to support IEEE 802.15.4g. We do that primarily because of the current unavailability of IEEE 802.11ah hardware. Please note that this “mimicking” approach has been utilized before (e.g., [22]). Specifically, Atmel AT86RF215 provides a partial support for a subset of the Modulation and Coding Schemes (MCSs) of IEEE 802.11ah (shown in Table 1), as shown in Table 2. In addition to the MCS, Atmel AT86RF215 allows altering the operational bandwidth at the physical layer. One of the supported options (referred to as option 1 in the OpenMote B data-sheet [28]) is to utilize the bandwidth of 1 MHz, i.e., the minimal bandwidth in IEEE 802.11ah (Table 1). The first three MCSs of the Atmel AT86RF215 radio (i.e., 0, 1, 2) use frequency repetitions (Table 2) and are therefore incompatible with IEEE 802.11ah. Hence, we only consider MCS 1 of IEEE 802.11ah, which corresponds with MCS 3 of the OpenMote B nodes’ Atmel AT86RF215 radio.

B. MEASUREMENT CAMPAIGN

The transmitter module continuously transmits packets of 509 bytes with 4 additional bytes for the Cyclic Redundancy Check (CRC) using IEEE 802.11ah. The transmitter sends ~ 32 packets per second, with the resulting throughput of 129 kbps. This is lower than the maximum physical-layer data rate supported by MCS 1, as shown in Table 1, in order not to overload the devices. Each time the transmitting OpenMote B

TABLE 1. IEEE 802.11ah MCSs [3].

MCS Index	Modulation	Coding rate	Data rate (kbps)	
			1 Mhz	2 Mhz
0	BPSK	1/2	300	650
1	QPSK	1/2	600	1300
2	QPSK	3/4	900	1950
3	16-QAM	1/2	1200	2600
4	16-QAM	3/4	1800	3900
5	64-QAM	2/3	2400	5200
6	64-QAM	3/4	2700	5850
7	64-QAM	5/6	3000	6500
8	256-QAM	3/4	3600	7800
9	256-QAM	5/6	4000	N/A
10	256-QAM	1/2 (x2)	150	N/A

TABLE 2. Selected OpenMote B (i.e., Atmel AT86RF215) MCSs.

MCS index	Modulation	Coding rate	Frequency repetition	Data rate (kbps)	802.11ah MCS
0	BPSK	1/2	4x	100	N/A
1	BPSK	1/2	2x	200	N/A
2	QPSK	1/2	2x	400	N/A
3	QPSK	1/2	No	800	1

sends a packet, the Raspberry Pi writes the packet number and current location to a log file. When the other module receives the packet, this message is logged to a computer over a serial interface. This second log contains the length of the packet, packet number, timestamp, SNR estimate, and the indication of the CRC correctness. The timestamps on the transmit and receive sides are then correlated for mapping of the received packets and their transmitting locations.

The measurement campaigns for both IEEE 802.11ah and IEEE 802.11n were carried out at the same urban area near the city of Antwerp, Belgium. The measurement area is depicted

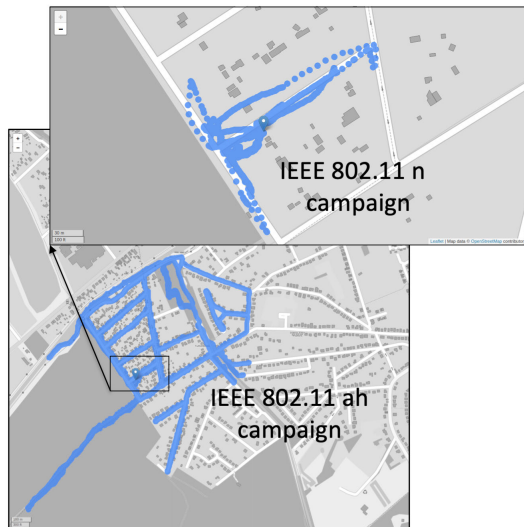


FIGURE 2. Measurement campaigns.

in Figure 2, containing primarily two to three-story residential buildings. The blue pins in Figure 2 (as well as later on in Figures 3, 4, 5a, and 7) indicate the location of the “access point” in the measurement campaigns. Moreover, note that the measurement campaigning area for IEEE 802.11n is in essence a sub-area of the IEEE 802.11ah campaign, merely due to the difference in the communication ranges featured by the two technologies.

The measurement campaign for IEEE 802.11ah took roughly 2.5 h, which resulted in a total of 341 280 packets sent and 121 658 of them received. Both receiving OpenMote B nodes used transceivers that reported RSSI as a signed integer between -127 and 4 (i.e., the -127 value indicates an invalid RSSI value, which never occurred during the tests). In addition, the transceivers reported the measured noise-floor, which was, in combination with the observed RSSI values, used for determining the SNR. Figure 2 gives an indication of the locations covered during the measurement campaign. The observed RSSI is shown in Figure 3a, while the packet loss is depicted in Figure 3b.

The method used in the campaign for IEEE 802.11n is similar to the one used for IEEE 802.11ah. In this case, the Raspberry Pi is used together with an existing AP, while the laptop is connected to the AP acting as the receiver. The Raspberry Pi sends a User Datagram Protocol (UDP) packet of about 500 bytes every 15 ms, thus about 66 packets are sent every second, achieving a throughput of 266 kbps (without taking the overhead of the network layers into account). The Raspberry Pi stores the current timestamp, location, and unique identifier of each packet that was sent. Moreover, it periodically (i.e. every 250 ms) logs the current location along with RSSI. The RSSI is obtained via the Linux `/proc/net/wireless` pseudo file on the Raspberry Pi. As the laptop logs each packet it receives, the packet loss (in 5 sec intervals) can be easily calculated. The measurements locations are also

depicted in Figure 2, while the observed RSSI and packet loss are shown respectively in Figure 4a and b. The IEEE 802.11n measurement campaign took 1 hour, during which 240 000 packets were sent and 204 203 of them were received.

C. EMULATION SETUP

The measurement campaign described above is not enough to evaluate the suitability of different vertical handover algorithms. There is also a need for user’s mobility in the environment of interest in order to invoke any of the algorithms in order to evaluate their performance. In this work, we enabled user’s mobility by means of emulation, i.e., by simulating the user walking at a normal walking speed and correlating its locations with the measurements obtained from the measurement campaign. By doing that, we were able to continuously switch between the two technologies based on the decisions made by the vertical handover algorithms. We have opted for an emulation-based study as it allowed us to compare the performance of all algorithms using exactly the same dataset obtained in the real-world scenario. This in turn enabled fully objective comparative performance evaluation of different algorithms, which would not have been possible through an experimentation-based study due to unavoidable small-scale temporal variability in the environment. Similar approaches for objective comparative benchmarking have been utilized for a variety of problems ranging from testing the performance of indoor localization systems [29], [30] to language [31] and image [32] recognition.

The simulated user’s walking trajectory is given in Figure 5, with the user moving at an average and maximum speeds of 4 and 6 km/h, respectively. The trajectory is roughly 5 km long and it takes about 75 minutes to complete. The distance to the AP, as shown in Figure 5b, illustrates that the device moves multiple times away from the AP. The other relevant emulation parameters are summarized in Table 3.

At different locations throughout the trajectory the locations are mapped to the RSSIs and packet losses observed during the measurement campaign. We have used k-d tree [33] for mapping between the locations on the one hand and RSSIs and packet loss at that location on the other. The packet loss was emulated using a function that decides to drop a packet in case the packet loss at the current location is higher than a random generated number [10]. For example, when the device is at a location where a 75% packet loss was measured, the function drops 75% of the packets sent by the server to the client, selected uniformly at random. When no such information is found, it re-executes the lookup but using a less granular lookup. The first lookup searches in an area of 310 m^2 whereas the fall-back lookup searches in an area of 1242 m^2 . If no data is found after the second lookup, the algorithm assumes that there is 100% packet loss at that location and thus all packets are dropped. The idea is that if 100 packets are sent, 75 of them will generate a random number lower or equal than 75, therefore resulting in the packet loss of 75%. This principle is often used for simulating Bernoulli processes [34].

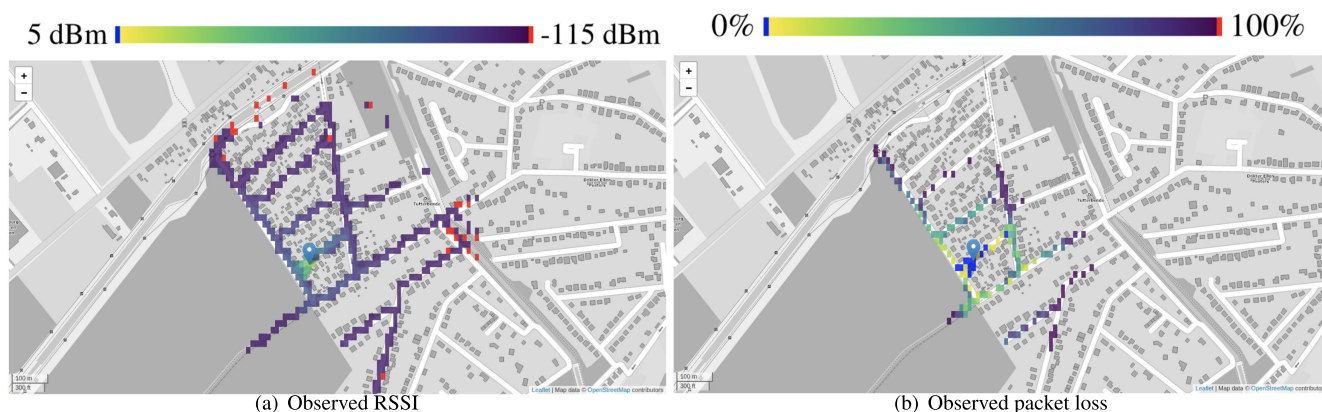


FIGURE 3. Observed RSSI and packet loss for IEEE 802.11ah.



FIGURE 4. Observed RSSI and packet loss for IEEE 802.11n.

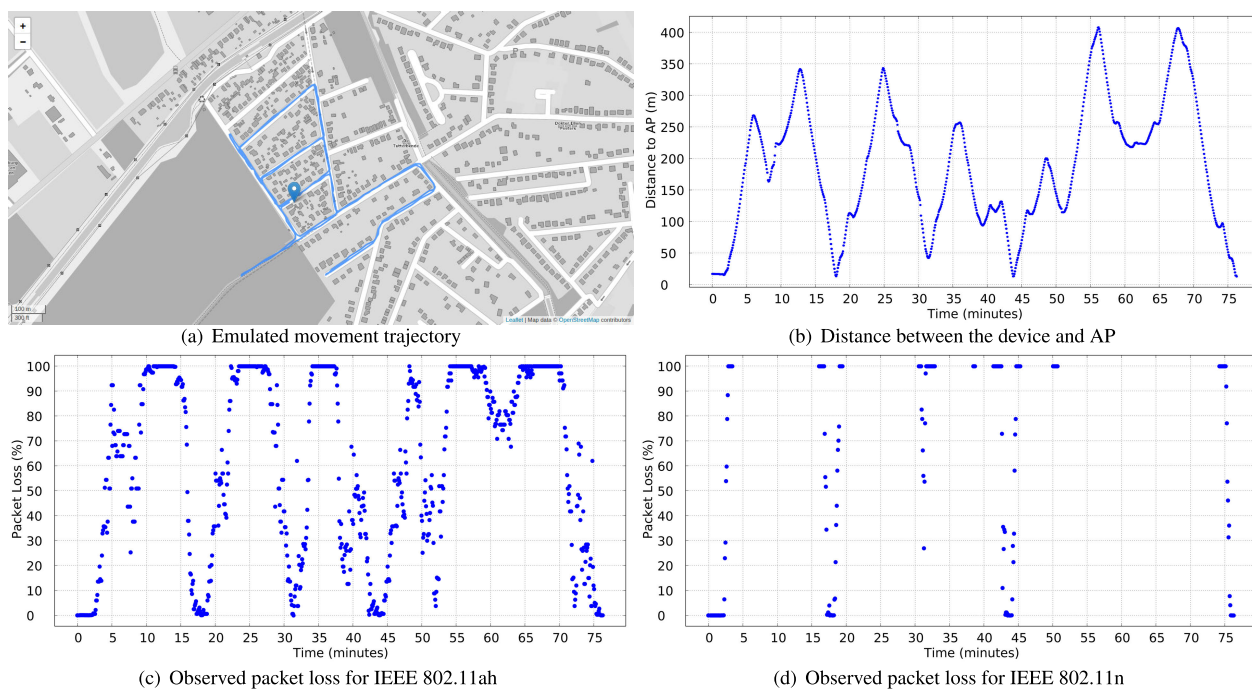


FIGURE 5. Overview of the emulation setup.

The emulated packet losses for the two technologies are depicted in Figure 5c and Figure 5d, which demonstrate that for large distances between the STA and AP both technologies experience connectivity loss, suggesting that the vertical

handover algorithms will be invoked for both technologies at certain points. The second part of the emulator is used in order to generate beacons. First of all, the average RSSI in an area of $310 m^2$ around the device’s current position is looked up.

TABLE 3. Parameterization of the considered algorithms.

Parameter	Value
Allowed number of missed beacon packets before disconnecting	3
Estimated localization error used as an internal parameter in the location-based algorithms	10 m
SNR threshold for establishing communication (all algorithms)	10 dB
Internal SNR threshold for optimizing the performance of the location-based algorithms	2 dB
Number of measurements used for creating the REM of the REM-based algorithm	121 658 / 204 203 (802.11ah / 802.11n)

If the RSSI is found in the data set, this implies that some packets were received during the measurement campaign, therefore a beacon must be sent. Finally, note that all the algorithms were internally parameterized (e.g., parameter β) to yield optimal performance for the considered environment, with more details provided in [10].

D. PERFORMANCE METRICS

- Packet Loss (PL): This metric indicates the observed packet loss during the whole experiment. It is calculated jointly for both technologies by taking into account the data and control packets sent from the client to the server and vice-versa. The metric gives an indication of the average quality of the established links.

$$PL [\%] = \frac{\text{Number of received packets}}{\text{Number of sent packets}} \quad (1)$$

- Ratio of successful data packets (Updates): In contrast to the previous metric, this one indicates the ratio between the successful data packets received by the server and the total number of such packets sent by the client. While the Connection Efficiency metric (see below) indicates how much time the device is connected, this metric shows how useful the connection is. For example, when the (absolute) connection time is high but the number of successful data packets is low, this means that the connectivity was not good enough to deliver data packets. Conversely, the connection quality is high when both the connection time is high and the number of successful data packets is high.

$$\text{Updates} [\%] = \frac{\text{Updates received by the server}}{\text{Updates sent by the client}} \quad (2)$$

- Radio On (On): this metric is the ratio of the total time the radio is turned on and the duration of the experiment and it is evaluated for each technology (i.e. IEEE 802.11ah and IEEE 802.11n). This metric indicates the energy consumption of the device, i.e., the longer the radio is on the more energy is consumed.

$$\text{On} [\%] = \frac{\text{Radio On}}{\text{Total Time}} \quad (3)$$

- Connection Efficiency (Eff): it is the ratio of the time the device is connected to this technology and the time the radio of this technology is powered on.

$$\text{Eff} [\%] = \frac{\text{Connected to Technology}}{\text{Radio On}} \quad (4)$$

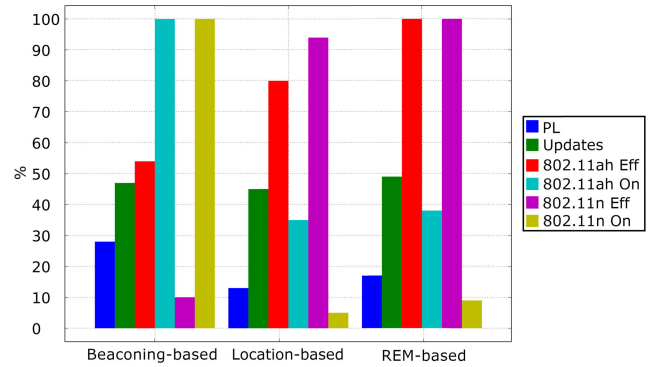


FIGURE 6. Performance achieved by different algorithms.

This indicates the efficiency of the radio that is used. If the ratio is low, it means that the radio has been turned on for too long (i.e., it was impossible to make a connection, even if the algorithm turned the radio on). On the other hand, when the ratio is high, the radio has been turned on only when a connection was actually possible. Even if this gives a good indication about the correctness of the algorithm, it should be noted that efficiency alone can be misleading. For example, if the radio is turned on 1% of the time and the device is connected the whole time, the efficiency is 100%. However, this does not necessarily represent a good result. Therefore, when looking at efficiency, the other metrics should be accounted for too.

- 95th percentile of distance between server and client (Distance): This final metric illustrates the maximum distance at which the client was able to successfully transmit a packet 95% of the time. Instead of using the absolute maximal distance, the 95th percentile is used in order to prevent the effect of outliers. The aim of this metric is to indicate the effects of different vertical handover algorithms on the achievable communication range.

V. EVALUATION RESULTS

Figure 6 depicts the performance of the considered algorithms observed during one iteration throughout the trajectory depicted in Figure 5a. As visible from Figure 6, the observed packet loss PL equals to 28, 13, and 16% for the beacon listening, location, and REM-based algorithms. In other words, both REM and location-based algorithms achieve significantly more reliable connectivity to either of the two technologies, as they yield roughly 45% and 55% lower packet loss compared to the beacon listening-based baseline. The main reason for this effect comes from the fact that the beacon listening-based algorithm relies on one technology as long as the beacons from that technology can be received, even if the STA is at the edge of the coverage region of the AP to which it is connected. This in turn results in an increase in the observed packet loss. Adversely, the other two algorithms make proactive location-based decisions about the potential handover to the second technology when the communication link with the first one is estimated to be relatively weak. In more general terms, the proactive



FIGURE 7. IEEE 802.11ah coverage achieved by different algorithms (95th percentile distance).

nature of the REM and location-based algorithms allows them to more optimally switch between the technologies, in turn substantially enhancing the reliability of communication.

Moreover, as visible in Figure 6, all of the considered algorithms achieve comparable performance in terms of the percentage of successfully delivered application-level updates from the client to the server, which is in the range between 45 and 50%. There are two effects influencing this metric. On the one hand, more reliable communication links achievable by the REM and location-based algorithms intuitively have a positive effect on the percentage of successfully delivered updates in comparison to the baseline. On the other hand, the baseline achieves better overall coverage (i.e., 95th percentile distance) than the other two algorithms, as depicted in Figure 7 for IEEE 802.11ah. The better coverage is the direct result of the both radio access interfaces being turned on during the whole experimentation run of the beacon listening-based baseline. The enhanced coverage of the baseline implies that at some locations (i.e., usually at the edge regions of both technologies), the REM and location-based algorithms will turn off both interfaces and would not be able to transmit any packets. Adversely, the baseline would be able to transmit some packets over relatively weak communication links, resulting in an increased percentage of successfully transmitted updates and balancing the effect of less reliable communication than the one achieved by the other two algorithms. However, this relatively small coverage-related benefit of around 10%, comes at a significant cost in terms of energy consumption of the STA.

In other words, the main benefits of the REM and location-based algorithms are visible from the Radio On (On) and Connection Efficiency (*Eff*) metrics. As visible in Figure 6, both radio access interfaces are turned on for the whole duration of the experiment for the baseline algorithm. In other words, beacon listening has to be performed periodically, even when the chance of establishing communication is rather low, resulting in the increase on the utilization of radio access interfaces. In contrast, the other two algorithms maintain the IEEE 802.11ah radio access interface on for

Algorithm 1: Beacon Listening-Based

```

Input: LinkType
Input: Allowed-Missed-Beacons
Global:Missed-Beacons = 0
for Beacon interval elapsed do
    Wake up to receive beacon for one beacon interval;
    if Beacon Received then
        Missed-Beacons = 0;
        if Already connected to Link then
            Advice = KeepLink;
        else
            Advice = PerformHandOver;
    else
        Missed-Beacons++;
        if Already connected to Link then
            if Missed-Beacons  $\geq$ 
                Allowed-Missed-Beacons then
                Advice = Disconnect;
            else
                Advice = KeepLink;
        else
            Advice = NoHandOver;
    MakeHandoverDecision(LinkType, Advice);

```

roughly 35-40% of the time, which represents an improvement of over 60% compared to the baseline. Similarly, the REM and location-based algorithms utilize the IEEE 802.11n interface for less than 10% of the overall experimentation time, yielding 10 times better performance than the baseline along this metric.

The reason for the discrepancy between the improvements yielded by the location and REM-based algorithms over the baseline for the two technologies (i.e., roughly 60% for IEEE 802.11ah and 10 times for IEEE 802.11n) can be found in the way we approached the measurement campaigns. As mentioned before and indicated in Figure 2, the measurement

Algorithm 2: Location-Based

```

Input: Required-SNR
Input: Locations of STA and APs
Input: COST-231 Hata parameters
Input: Allowed-Missed-Beacons
Input: LinkType
Global: Missed-Beacons = 0
for Beacon interval elapsed do
  if Not Already connected to Link then
    Estimated-SNR = Calculate estimated
    SNR(Locations of STA and APs, COST-231
    Hata parameters);
    if Estimated-SNR  $\geq$  Required-SNR then
      Wake up to receive beacon for one beacon
      interval;
      if Beacon received then
        Missed-Beacons = 0;
        if Actual-SNR < Required-SNR then
          | Advice = NoHandOver;
        else
          | Advice = PerformHandOver;
        end
      else
        | Advice = NoHandOver;
      end
    else
      | Advice = NoHandOver;
    end
  else
    Receive beacon during one beacon interval;
    if No Beacon received then
      Missed-Beacons++;
      if Missed-Beacons  $\geq$ 
      Allowed-Missed-Beacons then
        | Advice = Disconnect;
      else
        | Advice = KeepLink;
      end
    else
      Missed-Beacons = 0;
      if Actual-SNR < (Required-SNR) then
        | Advice = Disconnect;
      else
        | Advice = KeepLink;
      end
    end
  end
  MakeHandoverDecision(LinkType, Advice);
end

```

Algorithm 3: REM-Based

```

Input: Required-SNR
Input: Locations of STA
Input: REM
Input: Allowed-Missed-Beacons
Input: LinkType
Global: Missed-Beacons = 0
for Beacon interval elapsed do
  if Not Already connected to Link then
    Estimated-SNR = GetSurveyedSNR(Location
    of STA, REM);
    if Estimated-SNR  $\geq$  Required-SNR then
      Wake up to receive beacon for one beacon
      interval;
      if Beacon received then
        Missed-Beacons = 0;
        if Actual-SNR < Required-SNR then
          | Advice = NoHandOver;
        else
          | Advice = PerformHandOver;
        end
      else
        | Advice = NoHandOver;
      end
    else
      | Advice = NoHandOver;
    end
  else
    Receive beacon during one beacon interval;
    if No Beacon received then
      Missed-Beacons++;
      if Missed-Beacons  $\geq$ 
      Allowed-Missed-Beacons then
        | Advice = Disconnect;
      else
        | Advice = KeepLink;
      end
    else
      Missed-Beacons = 0;
      if Actual-SNR < (Required-SNR) then
        | Advice = Disconnect;
      else
        | Advice = KeepLink;
      end
    end
  end
  MakeHandoverDecision(LinkType, Advice);
end

```

campaign for IEEE 802.11n was performed in the sub-area of the IEEE 802.11ah measurement campaign area. In the later emulated walking trajectory that was defined throughout the IEEE 802.11ah measurement campaign area (cf., Figure 5a), the probability of successfully establishing communication with IEEE 802.11ah was, therefore, substantially higher than the same probability for IEEE 802.11n. The REM and

location-based algorithm were able to detect that and maintain their IEEE 802.11n radio access interfaces turned off for substantially longer periods of time compared to their utilizations of IEEE 802.11ah interfaces. Simultaneously, the radio access interfaces were continuously turned on for the beacon-listening baseline, yielding a discrepancy between the benefits for the two technologies.

Finally, the Connection Efficiency *Eff* metric demonstrates that proactive decisions made by the REM and location-based algorithms result in more optimal decisions on when to wake up a certain radio access interface. As visible in Figure 6, the REM-based algorithm achieves almost perfect efficiency, which is a direct result of having a large amount of REM data available for making accurate data-driven decisions. The efficiency of the location-based algorithm, which operates with significantly less input data and it is easier to deploy, is reduced by roughly 20% and 10% for respectively IEEE 802.11ah and IEEE 802.11n compared to the REM-based one. This is still significantly better than the efficiency achieved by the baseline, which is around 50 and 10% for IEEE 802.11ah and IEEE 802.11n, respectively.

VI. CONCLUSION

We have demonstrated the feasibility of performing location-based handovers between the IEEE 802.11ah-based Low-Power Wide-Area Networks (LPWANs) and IEEE 802.11n networks. We have done that by carrying out an extensive experimental evaluation of the performance of two location-based vertical handover algorithms, one based on the combination of physical location of the Station (STA) and an Radio Environmental Map (REM), and the other combining physical locations of the communicating devices and channel modeling. Our evaluation shows that the algorithms are able to achieve the coverage comparable to a beacon listening-based baseline, while reducing the utilization of the IEEE 802.11ah and IEEE 802.11n radio access interfaces by roughly a factor of 2 and 10, respectively. Given that the algorithm based on the combination of locations and channel modeling is easy to deploy (in contrast to the REM-based one), we find its performance particularly encouraging.

Future work will aim at further exploration of this hypothesis, primarily by evaluating the location-based algorithm in other setups and for different technologies. In terms of setups, we will focus on addressing what we see as the main limitations of this work. First, we will aim at evaluating the appropriateness of location-based handover for different operational modes of IEEE 802.11ah, mainly by considering different Modulation and Coding Schemes (MCSs). Given that the location-based handover algorithm can explicitly account for the desired SNR threshold above which communication establishment should be attempted, its operation can be easily “tuned” to make positive handover decisions at higher SNR thresholds, which in turn should suffice for supporting higher IEEE 802.11ah MCSs. In a similar way, the operation of the location-based algorithm can be continuously tuned to support adaptive IEEE 802.11ah MSCs. Moreover, we will consider different sources of location information, as well as different accuracy levels of those sources. Example-wise, IEEE 802.11ah will usually be used in outdoor environments that feature a certain Global Positioning System (GPS) accuracy, while IEEE 802.11n will mostly support indoor connectivity with lower accuracy of GPS-based localization. Similarly, it could happen that there

is no GPS available (e.g., due to indoor environment with no GPS connectivity or energy-related constraints of the devices) and the handover decision can be based only on less accurate localization source (e.g., LPWAN-based localization). It is worth emphasizing that the location-based handover algorithm is already able to explicitly account for different levels of inaccuracies of location information instances, even dynamically (e.g., change between indoor and outdoor environments, entering urban canyons, etc.), which we believe provides a solid ground for its further explorations along this aspect. An aspect we will consider is the dynamic adaptation of propagation models used by the algorithm based on the context in which the devices are positioned. For example, we will aim at accounting for an additional propagation loss if the STA enters a building or moves from one type of environment to another. Finally, in terms of other technologies, we will focus on LPWANs due to the significance of the “low-power” aspect in these technologies. We argue that the location-based algorithm, given that its design is primarily focused on energy minimization, could be particularly beneficial.

ACKNOWLEDGMENT

The computational resources were provided by the VSC (Flemish Supercomputer Center), funded by FWO and the Flemish Government - Department EWI.

APPENDIX

See Algorithm 1–3.

REFERENCES

- [1] *Wireless LAN Medium Access Control (MAC) and Physical Layer (PHY) Specifications Amendment 2: Sub 1 GHz License Exempt Operation*, IEEE Standard 802.11ah-2016s, May 2017, pp. 1–594.
- [2] U. Raza, P. Kulkarni, and M. Sooriyabandara, “Low power wide area networks: An overview,” *IEEE Commun. Surveys Tuts.*, vol. 19, no. 2, pp. 855–873, 2nd Quart., 2017.
- [3] L. Tian, J. Famaey, and S. Latre, “Evaluation of the IEEE 802.11ah restricted access window mechanism for dense IoT networks,” in *Proc. IEEE 17th Int. Symp. World Wireless, Mobile Multimedia Netw. (WoW-MoM)*, Jun. 2016, pp. 1–9.
- [4] S. Santi, L. Tian, E. Khorov, and J. Famaey, “Accurate energy modeling and characterization of IEEE 802.11ah RAW and TWT,” *Sensors*, vol. 19, no. 11, p. 2614, Jun. 2019.
- [5] J. Famaey, R. Berkvens, G. Ergeerts, E. D. Poorter, F. V. D. Abeele, T. Bolckmans, J. Hoebeke, and M. Weyn, “Flexible multimodal sub-gigahertz communication for heterogeneous Internet of Things applications,” *IEEE Commun. Mag.*, vol. 56, no. 7, pp. 146–153, Jul. 2018.
- [6] F. Lemic, A. Behboodi, J. Famaey, and R. Mathar, “Location-based discovery and vertical handover in heterogeneous low-power wide-area networks,” *IEEE Internet Things J.*, vol. 6, no. 6, pp. 10150–10165, Dec. 2019.
- [7] G. Caso, L. De Nardis, F. Lemic, V. Handziski, A. Wolisz, and M.-G.-D. Benedetto, “WiFi: Virtual fingerprinting WiFi-based indoor positioning via multi-wall multi-floor propagation model,” *IEEE Trans. Mobile Comput.*, vol. 19, no. 6, pp. 1478–1491, Jun. 2020.
- [8] J. Finnegan and S. Brown, “A comparative survey of LPWA networking,” 2018, *arXiv:1802.04222*. [Online]. Available: <http://arxiv.org/abs/1802.04222>
- [9] E. Khorov, A. Lyakhov, A. Krotov, and A. Guschin, “A survey on IEEE 802.11ah: An enabling networking technology for smart cities,” *Comput. Commun.*, vol. 58, pp. 53–69, Mar. 2015.
- [10] T. D. Koninck, “Experimental validation of location-based vertical handover algorithms in IEEE 802.11ah networks,” M.S. thesis, Dept. Comput. Sci., Univ. Antwerp, Antwerp, Belgium, 2020. Accessed: Mar. 1, 2021. [Online]. Available: https://medialibrary.uantwerpen.be/oldcontent/personalpage52077/files/final_version.pdf

- [11] R. D. Taranto, S. Muppirisetty, R. Raulefs, D. Sloock, T. Svensson, and H. Wymeersch, "Location-aware communications for 5G networks: How location information can improve scalability, latency, and robustness of 5G," *IEEE Signal Process. Mag.*, vol. 31, no. 6, pp. 102–112, Nov. 2014.
- [12] H. Celebi and H. Arslan, "Utilization of location information in cognitive wireless networks," *IEEE Wireless Commun.*, vol. 14, no. 4, pp. 6–13, Aug. 2007.
- [13] C.-C. Tseng, K.-H. Chi, M.-D. Hsieh, and H.-H. Chang, "Location-based fast handoff for 802.11 networks," *IEEE Commun. Lett.*, vol. 9, no. 4, pp. 304–306, Apr. 2005.
- [14] D. Sarddar, J. Banerjee, T. Jana, S. K. Saha, U. Biswas, and M. Naskar, "Minimization of handoff latency by angular displacement method using gps based map," *Int. J. Comput. Sci. Issues*, vol. 7, no. 3, pp. 29–37, 2010.
- [15] V. A. Siris and D. Kalyvas, "Enhancing mobile data offloading with mobility prediction and prefetching," *ACM SIGMOBILE Mobile Comput. Commun. Rev.*, vol. 17, no. 1, pp. 22–29, Jul. 2013.
- [16] G. G. L. Ribeiro, L. F. D. Lima, L. Oliveira, J. J. P. C. Rodrigues, C. N. M. Marins, and G. A. B. Marcondes, "An outdoor localization system based on SigFox," in *Proc. IEEE 87th Veh. Technol. Conf. (VTC Spring)*, Jun. 2018, pp. 1–5.
- [17] B. C. Fargas and M. N. Petersen, "GPS-free geolocation using LoRa in low-power WANs," in *Proc. Global Internet Things Summit (GIoTS)*, Jun. 2017, pp. 1–6.
- [18] Q. D. Vo and P. De, "A survey of fingerprint-based outdoor localization," *IEEE Commun. Surveys Tuts.*, vol. 18, no. 1, pp. 491–506, 1st Quart., 2016.
- [19] M. Aernouts, R. Berkvens, K. Van Vlaenderen, and M. Weyn, "Sigfox and LoRaWAN datasets for fingerprint localization in large urban and rural areas," *Data*, vol. 3, no. 2, p. 13, Apr. 2018.
- [20] F. Lemic, V. Handziski, G. Caso, L. De Nardis, and A. Wolisz, "Enriched training database for improving the WiFi RSSI-based indoor fingerprinting performance," in *Proc. 13th IEEE Annu. Consum. Commun. Netw. Conf. (CCNC)*, Las Vegas, NV, USA, 2016, pp. 875–881.
- [21] S. Santi, F. Lemic, and J. Famaey, "On the feasibility of location-based discovery and vertical handover in IEEE 802.11ah," in *Proc. IEEE Wireless Commun. Netw. Conf. (WCNC)*, May 2020, pp. 1–6.
- [22] T. De Koninck, S. Santi, J. Famaey, and F. Lemic, "Experimental validation of IEEE 802.11 ah propagation models in heterogeneous smart city environments," in *Proc. GLOBECOM-IEEE Global Commun. Conf.*, Taipei, Taiwan, Dec. 2020, pp. 1–6.
- [23] *COST Action 231, European Commission, and a. E. DGXIII Telecommunications, Digital Mobile Radio Towards Future Generation Systems*. Eur. Commission, Brussels, Belgium, 1999.
- [24] *Propagation Data and Prediction Methods for the Planning of Short-Range Outdoor Radiocommunication Systems and Radio Local Area Networks*. Standard Recommendation ITU-R P.1411-10, 2019.
- [25] A. Hazmi, J. Rinne, and M. Valkama, "Feasibility study of IEEE 802.11ah radio technology for IoT and M2M use cases," in *Proc. IEEE Globecom Workshops*, Dec. 2012, pp. 1687–1692.
- [26] Atmel Corporation. *Atmel AT86RF215 Device Family*. Accessed: Feb. 14, 2019. [Online]. Available: http://www.microchip.com/downloads/en/devicedoc/atmel-42415-wireless-at86rf215_datasheet.pdf
- [27] T. Watteyne, X. Vilajosana, B. Kerkez, F. Chraim, K. Weekly, Q. Wang, S. Glaser, and K. Pister, "OpenWSN: A standards-based low-power wireless development environment," *Trans. Emerg. Telecommun. Technol.*, vol. 23, no. 5, pp. 480–493, Aug. 2012.
- [28] X. Vilajosana, P. Tuset, T. Watteyne, and K. Pister, "OpenMote: Open-source prototyping platform for the industrial IoT," in *Proc. Int. Conf. Ad-Hoc Netw. Sanremo, Italy: Springer*, 2015, pp. 211–222.
- [29] N. Moayeri, M. O. Ergin, F. Lemic, V. Handziski, and A. Wolisz, "PerfLoc (Part 1): An extensive data repository for development of smartphone indoor localization apps," in *Proc. IEEE 27th Annu. Int. Symp. Pers., Indoor, Mobile Radio Commun. (PIMRC)*, Sep. 2016, pp. 1–7.
- [30] T. V. Haute, E. D. Poorter, F. Lemic, V. Handziski, N. Wirström, T. Voigt, A. Wolisz, and I. Moerman, "Platform for benchmarking of RF-based indoor localization solutions," *IEEE Commun. Mag.*, vol. 53, no. 9, pp. 126–133, Sep. 2015.
- [31] A. F. Martin and M. A. Przybocki, "NIST 2003 language recognition evaluation," in *Proc. 8th Eur. Conf. Speech Commun. Technol.*, 2003, pp. 1341–1344.
- [32] O. Russakovsky, J. Deng, H. Su, J. Krause, S. Satheesh, S. Ma, Z. Huang, A. Karpathy, A. Khosla, M. Bernstein, A. C. Berg, and L. Fei-Fei, "ImageNet large scale visual recognition challenge," *Int. J. Comput. Vis.*, vol. 115, no. 3, pp. 211–252, Dec. 2015.
- [33] J. L. Bentley, "Multidimensional binary search trees used for associative searching," *Commun. ACM*, vol. 18, no. 9, pp. 509–517, Sep. 1975.
- [34] S. Ross, "Generating discrete random variables," in *Simulation*, S. Ross, Ed., 5th ed. New York, NY, USA: Academic, 2013, ch. 4, pp. 47–68.



SERENA SANTI (Graduate Student Member, IEEE) received the M.Sc. degree in computer science from the University of Camerino, Italy, in 2016. She is currently pursuing the Ph.D. degree with the University of Antwerp, Belgium, affiliated with the Internet Technology and Data Science Lab (IDLab)—a Core Research Group of IMEC, Flanders. She is the author or coauthor of several publications in international journals and conference proceedings. Her main research interests include sub-GHz technologies and Internet of Things applications. She received a FWO SB scholarship, in 2017. She has received the Best Paper Award at WNS3 2018.

TOBIA DE KONINCK received the B.Sc. (Hons.) and M.Sc. (Hons.) degrees in computer science from the University of Antwerp, in 2018 and 2020, respectively.



GLENN DANEELS received the B.Sc. and M.Sc. degrees in computer science from the University of Antwerp, Belgium, in 2011 and 2013, respectively, and the M.Sc. degree in artificial intelligence from KU Leuven, Belgium, in 2014. He is currently pursuing the Ph.D. degree with the Internet and Data Lab (IDLab) Research Group—a Core Group of the Research Center IMEC, University of Antwerp. He is the coauthor of more than ten articles published in international peer-reviewed journals and conference proceedings. His main research interests include design, analysis and implementation of algorithms and protocols for low-power wireless sensor networks.



FILIP LEMIC received the B.Sc. and M.Sc. degrees from the University of Zagreb, in 2010 and 2012, respectively, and the Ph.D. degree (*magna cum laude*) from the Technische Universität Berlin, in 2017, supported by the German Academic Exchange Service (DAAD). From 2015 to 2016, he was a Visiting Researcher with the University of California, Berkeley, supported by the UC Berkeley's stipend for visiting scholars, and with the University of Michigan—Shanghai Jiao Tong University Joint Institute, from 2019 to 2020, supported by the Research Foundation Flanders (FWO). He is currently a Marie Curie Postdoctoral Researcher with the Internet Technology and Data Science Lab (IDLab), University of Antwerp, Belgium, and a collaborator with the NaNoNetworking Center in Catalunya (N3Cat), Universitat Politècnica de Catalunya, Spain. He is also a Senior Researcher with the IMEC Research Institute. He has coauthored more than 50 peer-reviewed scientific articles and has been involved in a number of international research projects, notably MSCA ScaleITN, EU EVARILOS, EU eWine, NIST's PerfLoc, and UC Berkeley's beyond-5G (xG).



JEROEN FAMAHEY (Senior Member, IEEE) received the M.Sc. and Ph.D. degrees in computer science from Ghent University, Belgium, in 2007 and 2012, respectively. Since 2016, he has been a Research Professor associated with IMEC and the University of Antwerp, Belgium. He has coauthored over 130 articles published in international peer-reviewed journals and conference proceedings. His research interests include wireless network optimization, low-power wireless communications, energy harvesting, and high-frequency mmWave and THz networking.